HHS Public Access

Author manuscript

J Immunol. Author manuscript; available in PMC 2017 January 01.

Published in final edited form as:

J Immunol. 2016 January 1; 196(1): 244–255. doi:10.4049/jimmunol.1403099.

The DNA ligase IV syndrome R278H mutation impairs B-lymphopoiesis via error-prone non-homologous end-joining[1]

Jihye Park[*,†], **Robert S. Welner**[‡], **Mei-Yee Chan**[*], **Logan Troppito**[*], **Philipp B. Staber**[‡], **Daniel G. Tenen**[‡], and **Catherine T. Yan**[*,†,‡,§]

[*]Department of Pathology, Beth Israel Deaconess Medical Center, Boston, MA 02215

[†]The Broad Institute of MIT and Harvard, Cambridge, MA 02143

[‡]Harvard Stem Cell Institute, Harvard Medical School, Boston, MA 02115

Abstract

Hypomorphic mutations in the non-homologous end-joining (NHEJ) DNA repair protein DNA Ligase IV (*LIG4*) lead to immunodeficiency with varying severity. Here, using a murine knock-in model, we investigated the mechanisms underlying abnormalities in class switch recombination (CSR) associated with the human homozygous Lig4 R278H mutation. Previously, we found that despite the near absence of Lig4 end-ligation activity and severely reduced mature B cell numbers, $Lig4^{R278H/R278H}$ ($Lig4^{R/R}$) mice exhibit only a partial CSR block, producing near normal IgG1 and IgE but substantially reduced IgG3, IgG2b and IgA serum levels. Here, to address the cause of these abnormalities, we assayed CSR in $Lig4^{R/R}$ B cells generated via preassembled IgH and IgK variable region exons (HL). This revealed $Lig4^{R278H}$ protein levels while intact exhibited a higher turnover rate during activation of switching to IgG3 and IgG2b; and delays in CSR kinetics associated with defective proliferation during activation of switching to IgG1 and IgE. Activated $Lig4^{R/R}$HL B cells consistently accumulated high frequencies of AID-dependent IgH locus chromosomal breaks and translocations, and were more prone to apoptosis, effects which appeared to be p53-independent as p53 deficiency did not markedly influence these events. Importantly, NHEJ instead of alternative end-joining (A-EJ) was revealed as the predominant mechanism catalyzing robust CSR. Defective CSR was linked to failed NHEJ and residual A-EJ access to unrepaired DSBs. These data firmly demonstrate $Lig4^{R278H}$ activity renders NHEJ to be more error-prone, and predict increased error-prone NHEJ activity and A-EJ suppression as the cause of the defective B-lymphopoiesis in Lig4 patients.

Introduction

Non-homologous end-joining (NHEJ) is one of two main DNA double strand break (DSB) repair pathways in mammalian cells. NHEJ exclusively repairs programmed DSBs that

[1]This work was supported by research funding from the ASH Scholar Award, NIH grant CA161151, V Foundation for Cancer Research Scholar Award, Emerald Foundation Young Investigator Award, Kimmel Scholar Award and startup funds to CTY.

[§]To whom correspondence should be addressed: Phone: 617-735-2459; Fax: 617-735-2480; cyan@bidmc.harvard.edu.

Author contributions: J.P. and C.T.Y. designed research; J.P., R.S.W., M.C., L.T., P.B.S., and C.T.Y. performed research; J.P., R.S.W., M.C., L.T., D.G.T. and C.T.Y. analyzed data; and J.P., R.S.W., and C.T.Y. wrote the paper.

Competing interest: The authors declare no competing financial interests.

occur in the context of lymphocyte-specific V(D)J recombination. Additionally, NHEJ plays key roles in the repair of general DSBs and is required for IgH class switch recombination (CSR) (1). CSR is a B-lymphocyte-specific event that changes a B cell's production of immunoglobulin from one class to another. This event is initiated from lesions introduced by the activation-induced cytidine deaminase (AID) protein into switch (S) regions, which are highly repetitive sequences that flank Immunoglobulin heavy chain (IgH) constant region exons (1, 2). These lesions are processed into DSBs and joined by NHEJ, which form junctions with either short microhomologies or no homology (3). In the absence of NHEJ, reduced by substantial CSR to all Ig isotypes (~25–50% of WT levels) is catalyzed by a predominantly microhomology-mediated alternative end-joining (A-EJ) repair mechanism (3). Seven proteins are involved in NHEJ (1), amongst which include DNA Ligase IV (Lig4), an ATP-dependent DNA ligase that has no other known functions outside of NHEJ (4).

In humans, hypomorphic mutations in the *LIG4* gene underlie the Lig4 Syndrome (5–11), a subset of Omenn Syndrome (12), Dubowitz Syndrome (13, 14), and radiosensitive SCID (13–17). Clinical features of the Lig4 patients include developmental growth retardation, often microcephaly; bone marrow (BM) abnormalities, radiohypersensitivity and predisposition to lymphoreticular malignancies for certain mutations; and the development of immunodeficiency (early to late onset, often initially unrecognized) associated with mild to severe defects in V(D)J recombination and CSR (7, 11, 14, 18). Many of these phenotypes overlap with clinical features of other DNA repair deficient syndromes, particularly Nijmegen Breakage Syndrome, and also Fanconi anemia and Bloom's syndrome (7, 14, 18). To date, 16 genetically inherited hypomorphic *LIG4* mutations from 29 patients have been described (11, 16). These mutations are found in homozygous or compound heterozygous states. The variability in the phenotypes of Lig4 patients has been attributed to differences in mutational impacts on Lig4 protein stability and function, with the more deleterious mutations resulting in earlier mortality (11, 16).

In the first reported case of the Lig4 Syndrome, a hypomorphic homozygous missense *LIG4* mutation that lies within the conserved KxDGx**R** active site (arginine to histidine 278; R278H) was identified in a developmentally normal 14 year-old patient (180BR) with T-cell acute lymphoblastic leukemia (T-ALL) (5). During treatment for leukemia, indicative of latent immune dysfunctions, the patient became severely thrombocytopenic and leucopenic post chemotherapy; and indicative of defective DNA repair, exhibited severe radiohypersensitivity and morbidity in response to radiation treatment (5). The homozygous R278H mutation impairs DSB rejoining by severely compromising but not abrogating the ligase-AMP enzyme-adenylate complex formation and nick ligation activities of the mutant Lig4 protein, but its double strand DNA binding activity and interactions with XRCC4, which stabilizes and protects Lig4 from degradation, remain intact (6, 9, 19, 20). Our group generated mice harboring targeted knock-in of the $Lig4^{R278H/R278H}$ mutation to mimic this patient's disease (which we refer to as $Lig4^{R/R}$) (21). The $Lig4^{R/R}$ mice represent the first model of a naturally occurring Lig4 Syndrome mutation (21). In mice, *LIG4* deficiency is embryonic lethal, and is associated with severe developmental growth defects and massive neuronal apoptosis due to activation of p53-dependent response to unrepaired DSBs (4);

which could be rescued by simultaneous p53 deficiency but predisposed young adult $Lig4^{-/-}p53^{-/-}$ mice to aggressive pro-B lymphomas (22). In $Lig4^{R/R}$ mice, only the activity of the Lig4 protein (similar to in the 180BR patient) is severely affected (21); and they appear to model the complex cellular and clinical phenotype of Lig4 Syndrome patients (21). These include developmental growth retardation and a reduced lifespan; severe cellular radiosensitivity and increased cancer predisposition, particularly to T cell malignancies (characteristic of the $Lig4^{R278H/R278H}$, 180BR patient); impaired V(D)J recombination and incomplete defects in T and B lymphopoiesis, the latter associated with the progressive loss of B cells starting from the progenitor stage in the BM; and despite a scarcity of splenic B cells, only a partial block in CSR (21).

The molecular impact of the Lig4 R278H mutation on mature B cell functions has not been previously investigated. Here, to address this, we intercrossed into $Lig4^{R/R}$ mice, pre-assembled immunoglobulin heavy chain (23) and κ light chain (24) knock-in alleles (collectively referred to as “HL”), singly and in combination with a p53 knockout allele (25), to directly assess the impact of $Lig4^{R278H}$ activity on mechanisms of DNA damage response and repair in peripheral B cells during CSR.

Materials and Methods

Mouse strains and cell lines

$Lig4^{R/R}$HL mice were obtained by breeding $Lig4^{R/+}$ (21) with IgH B-18-HC (23) and Igκ 3–83k-LC knock-in (HL) mice (24), with the HL alleles bred to homozygosity as described (3, 26). $Lig4^{R/R}p53^{-/-}$HL mice were generated by intercrossing $Lig4^{R/+}$HL and $p53^{-/-}$ mice. All experiments were carried out with cohort littermates between 5–7 weeks (wks) of age. All mice were maintained in an AALAC and IACUC approved BL1 animal facility at the Beth Israel Deaconess Medical Center.

Western blotting

Cultured cells were lysed with RIPA buffer (50 mM of Tris-HCl, pH 8.0, 150 mM of NaCl, 1% of NP-40, 0.5 % of deoxycholate, 0.1% of SDS) containing phosphatase inhibitor cocktail (Roche) and protease inhibitor cocktails. Lysates were subjected to western blotting with antibodies against Lig4 (27) and β-actin (Cell Signaling) as described (3).

Splenic B cell purification and *in vitro* culture

$CD43^{-}$ splenic B cells were isolated subsequent to RBC lysis (Sigma) by negative selection using CD43 (Ly-48) Microbeads (Miltenyi), and cultured with α-CD40+IL4, LPS+α-IgD and RP105 as described (3).

Cell proliferation, CFSE and cell cycle analysis, and apoptosis assay

Proliferation of cultured B cells were quantified daily with Trypan Blue staining to exclude dead cells (Sigma). For CFSE tracking, splenic B cells were purified and incubated with 5 μM carboxyfluorescein diacetate succinimidyl ester (CFSE) for 5 min at 37°C and cultured as previously described (3). Cell cycle profile was analyzed by Propidium Iodide (PI) staining. Briefly, cells were fixed in 70% ice-cold ethanol, resuspended in PBS containing

50 μg/ml of PI and 50 μg/ml of Ribonuclease A (Sigma), and subjected to FACS analysis, the cell cycle distribution evaluated based on DNA content using the FlowJo Modfit LT cell cycle analysis platform. Apoptosis was measured by FACS analysis of Annexin-V staining, performed according to the manufacturer's protocols (BD Bioscience Parmingen). BM cells were stained with Annexin-V-FITC and DAPI as described (28).

Measurement of protein half-life

WTHL and Lig4$^{R/R}$HL B-lymphocytes stimulated with α-CD40+IL4 or LPS+α-IgD were treated with cycloheximide at 50 μg/ml, and harvested at 12h and 24h. Samples were lysed with RIPA buffer (50 mM of Tris-HCl, pH 8.0, 150 mM of NaCl, 1% of NP-40, 0.5 % of deoxycholate, 0.1% of SDS) with phosphatase inhibitor cocktail (Roche) and protease inhibitor cocktails. Lysates were subjected to western blotting with antibodies against Lig4 and β-actin as described (3).

ELISA

Ig serum levels and supernatant IgM and IgG isotypes from cultured supernatants, obtained 96 h (4 days) after stimulation were performed using isotype-specific antibodies against IgM, IgG1, IgG2b, IgG3, IgA (Southern Biotechnology Associates), and IgE (BD Pharmingen) as described (3).

CSR Switch region junction analysis

Sμ–Sγ1, Sμ–Sε and Sμ–Sα junctions were amplified by PCR from genomic DNA prepared directly from splenocytes or from CD43^{-} B cells activated with α-CD40+IL4 or LPS+α-IgD for 96 h as described (3, 29, 30).

Two-color IgH-FISH, Telomere-FISH

Metaphases were prepared after 96 h of activation in α-CD40+IL4 or LPS+α-IgD and processed as described (3, 31).

Confocal microscopy

Activated B cells were cytospun, fixed, and permeabilized and cells were incubated with 53BP1(Novus, NB100-904) antibody followed by incubation with secondary antibody (Alexa Fluor 488 goat anti-rabbit IgG) and counterstained with DAPI to detect nuclei as described (45). Images were acquired on Zeiss LSM510 Meta Upright Confocal Microscopy.

Flow cytometry

Antibodies used: B220 (RA-3-6B2), CD19 (6D5), Annexin-V from Biolegend, CD43 (S7), IgG1 (A85-1) from BD Bioscience, IgM (11E10), IgG3 (B10) and CD95 (clone Jo2) are from Southern Biotech. All assays were run on LSRII SORP (BD Bioscience) with 5 lasers and the FACS data analyzed by using FlowJo version. 9.7.6.

Statistics

Unpaired Student's t test on means ± standard deviations (error bars). n indicates the numbers of independent experiment performed.

Results

Partial restoration of Lig4$^{R/R}$ B-lymphocytes by HL knock-in alleles

Lig4$^{R/R}$ mice have profound B cell abnormalities that include substantial reductions in B220^{+}IgM^{-}CD43^{+} progenitor B cells in the BM and a scarcity of mature B220^{+}IgM^{+}CD43^{-} B cells in the spleen (21). Because of low numbers of splenic B cells observed in Lig4$^{R/R}$ mice (Fig. 1A, upper panel), to test the impact of the homozygous Lig4 R278H mutation on proliferation and CSR, we intercrossed pre-assembled IgH B-18-HC (23) and Igκ 3–83k-LC knock-in alleles (24) (HL) to homozygosity into the Lig4$^{R/R}$ mouse strain, generating Lig4$^{R/R}$HL mice. The HL knock-in bypasses the requirement for V(D)J recombination to directly generate splenic B220^{+}IgM^{+}CD43^{-} B cells shown to undergo normal CSR (3, 26, 32), including in RAG1/2-deficient mice (33). Notably, Lig4$^{R/R}$HL mice frequently became moribund of an unknown cause after 8 wks of age (data not shown). As such, all B cell analyses were performed between ~5–7 wks of age. Flow cytometric (FACS) analysis showed the percentages of splenic B220^{+}IgM^{+} B-lymphocytes in Lig4$^{R/R}$HL mice were restored to WT levels (Fig. 1A, lower panel), but total cell counts showed only partial restoration of the steady state peripheral B cell pool to ~2–3×10^{6}/mouse, ~20% of WT levels (Fig. 1B), with no detectable increase in either splenic or lymph node cellularity (Fig. 1C). We found this is because the Lig4$^{R/R}$HL splenic B220^{+}IgM^{+} B-lymphocytes are more prone to apoptosis, which was evidenced by increase in the percentage of Annexin-V^{+} mutant splenocytes spanning early to late apoptotic stages (Fig. 1D–1E). To test if the reduction in Lig4$^{R/R}$HL peripheral B-lymphocyte numbers under steady-state conditions is due to activation of a p53-dependent apoptotic response, we generated Lig4$^{R/R}$p53$^{-/-}$ HL mice. FACS analysis showed that compared to Lig4$^{R/R}$HL mice, loss of p53 activity had little impact on the splenic B220^{+}CD43^{-}IgM^{+} B-lymphocyte numbers (Fig. 1F), indicating this apoptotic response is p53-independent. ELISA quantification of the serum Ig levels of 5–7 week old Lig4$^{R/R}$HL mice, compared to age-matched WTHL cohorts, showed that while relatively normal levels of IgM, IgG1 and IgE were detected, like Lig4$^{R/R}$ mice (21), the serum IgA level of Lig4$^{R/R}$HL mice was significantly reduced (Fig. 1G). These findings suggest these CSR abnormalities might be due to specific impacts of the mutant Lig4^{R278H} activity on NHEJ functions during CSR instead of a general impact on peripheral B cell survival.

Impaired proliferation and CSR kinetics in Lig4$^{R/R}$HL B cells attempting IgG1 but not IgG3 switching

CSR *in vivo* is stimulated by both T cell-dependent and independent antigens, which can be mimicked *in vitro* by activating B cells with anti-CD40 plus IL-4 (α-CD40+IL4) to stimulate class switching to IgG1 and IgE; and LPS plus anti-IgD (LPS+α-IgD) to stimulate class switching to IgG2b and IgG3 (2, 34). To evaluate the impact of the mutant Lig4^{R278H} activity on NHEJ functions during CSR, Lig4$^{R/R}$HL, WTHL and AID$^{-/-}$ (as a negative control for CSR) splenic IgM^{+}CD43^{-} B cells were activated in α-CD40+IL4 or LPS+α-IgD.

Previously we reported a 5 to 10-fold reduction in the Lig4 protein in $Lig4^{R/R}$ thymocytes (21), whereas the levels of the protein in the 180 BR patient fibroblast line were reportedly comparable to in control 1BR fibroblast line (6). Western blotting showed comparable levels of Lig4 protein expression in α-CD40+IL4 and LPS+α-IgD activated $Lig4^{R/R}$HL and WTHL B cells (Fig. 2A). However, examination of half-life of the Lig4 protein showed the turnover rate of the $Lig4^{R278H}$ was faster than WT Lig4 in LPS+α-IgD, but indistinguishable from WT Lig4 in α-CD40+IL4 (Supplemental Fig. 1A). To assess if the difference in protein turnover might be correlated to differences in cell proliferation, daily cell counts was performed. This revealed a severe defective in proliferative expansion of $Lig4^{R/R}$HL B-lymphocytes when activated in α-CD40+IL4 (Fig. 2B) whereas their proliferation in LPS+α-IgD was at near WT levels (Fig. 2C). To further examine the rate of cell division in these activated cells, cells were labeled with carboxyfluorescein diacetate succinimidyl ester (CFSE) dye and measured by flow cytometry following dye dilution. This revealed the defect in proliferation in α-CD40+IL4 for $Lig4^{R/R}$HL B cells was accompanied by defect in cell division as shown by the lag in CFSE dilution peaks compared to WTHL B cells (Fig. 2D), whereas the CFSE dilution peaks of WTHL and $Lig4^{R/R}$HL B cells in LPS +α-IgD mostly overlapped (Fig. 2E). This led us to compare the cell cycle profile of $Lig4^{R/R}$HL B-lymphocytes in these two activating conditions. This was accomplished by FACS analysis of activated cells stained with propidium iodide (PI), which reveals their DNA content. PI staining, assessed at 72 h, 96 h and 108 h time points revealed the cell cycle profile of $Lig4^{R/R}$HL B-lymphocytes was comparable with control cells in both activating conditions, indicating the proliferation differences are not due to a specific cell-cycle checkpoint defect (Supplemental Fig. 1B and 1C).

To determine if the kinetics of class switching in $Lig4^{R/R}$HL versus WTHL B cells activated with α-CD40+IL4 versus LPS+α-IgD might also be affected, class switching respectively to IgG1 and IgG3 was examined by FACS at 12 hour (h) intervals from 60 h to 120 h (day 2.5 to day 5) of activation. Activated cultures were maintained at a density of 0.5–1×10^6cells/ml. Additionally, supernatants were taken on day 4 (96 h) of activation for ELISA quantification of secreted antibody levels. FACS analysis revealed $Lig4^{R/R}$HL B-lymphocytes to undergo robust, switching to IgG1 (Fig. 3A). Importantly, the time course assay of IgG1 switching from 60 h to 120 h of activation revealed $Lig4^{R/R}$HL B-lymphocytes to undergo dramatically delayed kinetics of IgG1 switching, that resulted in ~80% to near WT levels of IgG1 switching at late time points, after CSR in control cells had already plateaued (Fig. 3B). This was confirmed by supernatant ELISA from α-CD40+IL4 cultures that showed near WT levels of IgG1 and IgE (Fig. 3C). By contrast, IgG3 switching of $Lig4^{R/R}$HL B-lymphocytes was severely reduced (~90–96% reduction) and did not increase at later time points (Fig. 3D–E). This was also confirmed by supernatant ELISA from LPS+α-IgD cultures that showed significant reductions in IgG3 and IgG2b (Fig. 3F); data that correlated with the levels of serum IgG3 and Ig2b detected previously in $Lig4^{R/R}$ mice (21). These findings are in contrast to mice with another *LIG4* mutation ($Lig4^{Y228C/Y228C}$), in which Lig4 protein levels were nearly absent (35). In $Lig4^{Y228C/Y228C}$ B-lymphocytes, proliferation in LPS (including LPS+IL-4) instead of α-CD40+IL4 conditions was impaired, and switching to both IgG1 and IgG3 were both significantly reduced, similar to Lig4-deficient B-lymphocytes (35). This raised the question as to

whether the impaired proliferation of Lig4$^{R/R}$HL B-lymphocytes in α-CD40+IL4 might be specific to α-CD40 culturing conditions. To test this, we stimulated Lig4$^{R/R}$HL B-lymphocytes with LPS+IL4, which also activates class switching to IgG1 and IgE. This revealed the proliferative expansion of Lig4$^{R/R}$HL B-lymphocytes in LPS+IL4 was severely compromised, similar to in α-CD40+IL4 (data not shown), demonstrating their reduced proliferation during IgG1 and IgE switching is not activation-specific. Moreover, p53-deficiency in Lig4$^{R/R}$p53$^{-/-}$HL B-lymphocytes also failed to increase the level of IgG1 or IgG3 class switching (Supplemental Fig. 2A and 2B). Altogether these results suggest that the slower CSR kinetics is more likely associated with slower end-joining activity of the Lig4^{R278H} protein and not cell death caused by activation of the p53-dependent response.

Lig4$^{R/R}$HL B cells frequently generate IgH chromosomal breaks and translocations

Decreased CSR in NHEJ-deficient B-lymphocytes is normally equated with an end-joining defect resulting in increased levels of IgH-locus breaks (3, 32). Therefore, we performed metaphase fluorescent in situ hybridization (FISH) using bacterial artificial chromosome (BAC) probes containing genomic sequences flanking the 5′ and 3′ ends of the IgH locus to assay for IgH-specific breaks generated during B cell activation; and additionally, assayed for the overall DNA breaks using telomere-specific probes (T-FISH) (3). IgH FISH analysis revealed the substantial levels of breaks in the IgH locus (~ranging 38–58%) in α-CD40+IL4 activated Lig4$^{R/R}$HL B-lymphocytes (Fig. 4A and 4B; Table 1). T-FISH analysis further revealed that these breaks were primarily chromosomal breaks, which were generated during the pre-replicative phase of the cell cycle (Fig. 4C; Table 1). The majority of IgH-specific breaks involved both IgH loci with nearly 40% joined in translocations, either in chr12-chr12 dicentric or to other chromosomes (Fig. 4D; Table 1). Strikingly, in LPS+α-IgD, in which CSR is severely impaired, substantial levels of IgH chromosomal breaks (averaging ~30%) and translocations were detected in Lig4$^{R/R}$HL (Fig. 4B, 4D) and also in Lig4$^{R/R}$p53$^{-/-}$HL B-lymphocytes (Fig. 4E). Interestingly, the levels of breaks appeared to be equivalent between these groups, indicating cellular p53 status does not impact the frequency of these events in the homozygous Lig4 R278H mutant setting. The substantial levels of IgH breaks in both activating conditions suggest the Lig4^{R278H} activity results in slower, more error-prone DSB repair. Supporting this notion was evidence of the persistence of 53BP1 foci in activated Lig4$^{R/R}$HL B-lymphocytes (Fig. 4F, 4G). Moreover, failure of p53 to rescue survival of naïve or activated Lig4$^{R/R}$p53$^{-/-}$HL B-lymphocytes (Fig. 4E), and increase in sub-G1 population in Lig4$^{R/R}$HL B-lymphocytes during activation (Supplemental Fig. 1B, 1C) indicated the majority of these DSBs remain unrepaired and are eliminated via a p53-independent mechanism, which based on normal FAS surface expression is unlikely to be FAS-mediated (Supplemental Fig. 1D).

Because Lig4$^{R/R}$ mice spontaneously produce autoantibodies (21), we considered the possibility that a subset of their IgH breaks could be catalyzed by the RAG endonuclease during V(D)J recombination similar to in ATM$^{-/-}$ mice (36), or via a secondary V(D)J recombination event in the periphery (37, 38). To test this, Lig4$^{R/R}$HL B-lymphocytes were cultured with antibody against the toll-like receptor CD180 (RP105), which triggers proliferative expansion without inducing AID expression and CSR (36). The near absence of

IgH breaks in RP105-cultured Lig4$^{R/R}$HL B-lymphocytes (Fig. 4B, Table 1) confirmed that those detected in CSR assays were indeed AID- and not RAG-mediated.

Lig4^{R278H} activity limits CSR catalyzed by A-EJ

Previously, analysis of CSR joins obtained from the peripheral blood of Lig4 2304 and 411BR patients harboring compound heterozygote truncating R580X/R814X, and homozygous R278H;A3V;T91 mutations respectively, showed IgA switching in both patients to result from joining longer base-pair overlaps (microhomologies, MH) at Sμ-Sα, with sequence bias towards joining within particular regions of Sμ donor and Sα acceptor sites—indicative of the predominance of A-EJ in their repair (18). By contrast, 1-bp nucleotide insertions but no MH were found at Sμ-Sγ CSR junctions (18). Notably, despite sharing the homozygous R278H mutation with the 180BR patient, the 411BR patient was phenotypically distinct, and like the 2304 patient, displayed microcephaly, developmental delay, immunodeficiency and no evidence of cancer (9). Also, although Lig4 protein was intact in 411BR fibroblasts while nearly undetectable in 2304 patient fibroblasts, unlike the 180BR homozygous R278H mutation, both the 411BR and 2304 mutation combinations abolished Lig4 nick ligation and adenylation activities (9). It remains unclear as to why IgA versus IgG switch junctions were resolved so differently in these two hypomorphic Lig4 mutant settings, and the relevance of DSB repair mechanisms to the phenotypic disparities. Different A-EJ mechanisms, one that recombines via MH at Sμ-Sα regions and another that introduces nucleotide insertions at Sμ-Sγ regions was proposed to catalyze CSR when NHEJ is impaired in these mutant settings (18). While in normal controls, CSR was proposed to involve multiple DSB repair pathways, dominant (NHEJ) and alternative, to resolve the initial lesions in different S regions (18). Currently, although it is clear that A-EJ is distinct and robustly catalyzes CSR in the complete absence of NHEJ, its contribution to DSB repair when NHEJ factors are intact but residually functional, as might be expected in the 180BR patient setting, remains unclear. There is also no report on the study of the180BR patient's B-lymphocytes (5).

To address this, we asked if DSB repair is biased towards A-EJ or still catalyzed by NHEJ, and if differences in DSB repair pathway choice based on dependence on junctional homology could account for the partial CSR block in the Lig4$^{R/R}$ mice. The highest sequence homology is shared by Sμ with Sε and Sα region sequences (39). Therefore to address these questions, we analyzed the pattern of junctional homology in Sμ-Sγ1, and Sμ-Sε compared to Sμ-Sα joins, which we obtained by nested PCR from genomic DNA of activated Lig4$^{R/R}$HL B-lymphocytes and unactivated Lig4$^{R/R}$ splenocytes, as compared to WT(HL) controls. As previously shown, classical NHEJ joins both direct/blunt ends and ends with short donor/acceptor microhomology (MH), while A-EJ almost exclusively joins via junctional homology and trends towards longer MH (3). We found the predominant pattern of junctional (1–4bp) homologies in mutant Sμ-Sε and Sμ-Sγ1 junctions were normal, involving both direct and MH joins, characteristic of NHEJ, with very few sequences containing the long MH that are characteristic of A-EJ; and the frequency of junctions with nucleotide (nt) insertions obtained were within normal ranges (Fig. 5A–5C; Table 2; Supplemental Fig. 3A–3B). These findings demonstrate the predominance of NHEJ in the robust IgE and IgG1 switching. By contrast, we found mutant Sμ-Sα junctions

resulting from the reduced switching to IgA in Lig4$^{R/R}$(HL) mice (Fig. 1G) were predominantly biased towards MH joining (23 out of 24 total joins analyzed) (Supplemental Fig. 3C; Table 2). However, the severe reduction in mutant Sμ-Sα blunt joins is unlikely due to a specific A-EJ MH bias, since Sε region shares a similar level of homology as Sα to the Sμ region (~70%) (1, 39), and CSR to IgE remain intact in Lig4$^{R/R}$(HL) mice. More likely, residual A-EJ access to unrepaired lesions in Sμ and Sα regions involves increased turnover mutant Lig4^{R278H} protein, as found in LPS+α-IgD (Supplemental Fig. 1A, right panel), wherein rapid displacement of the mutant Lig4^{R278H} protein and associated NHEJ factors could explain the severe impairments in IgA (likely also IgG3 and IgG2b) switching. These findings support the notion that the mutant Lig4^{R278H} activity inhibits access of double strand (ds) DNA substrates that favor A-EJ.

Additionally, the distribution of DSBs in Lig4$^{R/R}$ Sμ donor, and Sα and Sε acceptor sites were widely distributed, indicating a lack of repair sequence bias (Fig. 5A–5B). Finally, whereas somatic mutation was shown to be less frequent in 2304 and 411BR patient cells, a finding that had suggested a role for Lig4 in the generation of somatic mutations during antibody diversification in human (18), the frequency of somatic mutations spanning all Lig4$^{R/R}$(HL) mutant CSR joins analyzed was within normal ranges (Supplemental Table 1), similar to our previous data for Lig4$^{-/-}$ and Xrcc4$^{-/-}$ B-lymphocytes (3, 32). We speculate this might reflect differences in hypomorphic *LIG4* mutation impacts on B cell repertoire and peripheral B cell survival.

Discussion

The Lig4$^{R/R}$ mouse strain is the first model of the naturally occurring human homozygous Lig4 R278H disease allele. In this study, we provide detailed analysis of the impact of the mutant Lig4^{R278H} activity on DNA damage response and genomic stability during CSR. Our findings show Lig4$^{R/R}$ B-lymphocytes are more prone to apoptosis in a p53-independent manner, as cellular p53 status had little effect on their proliferation and survival, or the frequency of IgH chromosomal breaks and translocations. Furthermore, the substantial levels of unrepaired IgH chromosomal breaks and translocations, and the persistence of 53BP1 foci in activated Lig4$^{R/R}$HL B-lymphocytes demonstrated a slower rate of DSB repair that is more error-prone. Moreover, the predominance of direct and MH joins in the robust CSR to IgG1 and IgE, and MH joining in the defective CSR to IgA, demonstrated A-EJ to be largely suppressed, while NHEJ is the predominant DNA repair pathway catalyzing CSR with this Lig4 mutation.

These findings raise several interesting questions to be addressed. Most importantly will be to better understand how normal Lig4 and NHEJ activity suppresses A-EJ, and if changes in the balance between utilization of NHEJ versus A-EJ underlie the complexity of phenotypes in Lig4 patients. Unlike Lig4$^{Y288C/Y288C}$ mouse model, which showed severely reduced Lig4 protein expression (35), our analysis of activated Lig4$^{R/R}$HL B-lymphocytes shows they have intact Lig4 protein expression in steady state. This result, together with the predominance of NHEJ catalyzing CSR in activated Lig4$^{R/R}$HL B-lymphocytes, suggests that despite only residual end-ligation activity, the presence of normal levels of the Lig4^{R278H} protein is sufficient to restrict A-EJ from gaining access to unrepaired DSBs. In

this context, whereas faster proliferation has been linked to optimal IgH class switching, activated Lig4$^{R/R}$HL B-lymphocytes showed defective proliferation and CSR kinetics yet robust IgG1 switching. Our evidence suggests this to be a direct consequences of residual but intact Lig4-NHEJ mediated ds DNA binding and repair, and not increased participation of A-EJ. Furthermore, impaired switching to IgG3 (also IgG2b, IgA) is most likely a consequence of additional involvement of accumulated cytotoxic DNA damage under conditions in which NHEJ activity is displaced by more rapid turnover of the mutant Lig4^{R278H} protein, as observed in the LPS+α-IgD cultures; thereby allowing residual A-EJ access to a subset of unrepaired DSBs. This indeed appears to be the case for IgA switching in Lig4$^{R/R}$ mice; and is consistent with previous human 2304 and 411BR *LIG4* mutation data that showed IgA switching was largely micro-homology mediated (18). We propose the effect on Lig4 protein turnover and impacting A-EJ access, as opposed to a specific IgH isotype donor/acceptor homology dependence, as the major cause of the partial CSR block within this *LIG4* mutation. For instance, increased apoptosis due to decreased NHEJ activity, caused by more rapid turnover of Lig4^{R278H} and other NHEJ factors during attempted IgG3, IgA, and IgG2b switching could explain their reduced production under LPS conditions and *in vivo* in Lig4$^{R/R}$ mice.

Our overall data provide strong evidence that residual functional Lig4 activity, if not more rapidly displaced, is sufficient to cause NHEJ to preclude A-EJ as long as its DSB binding activity is intact. This may also be true for its interacting partner, Xrcc4. However since other NHEJ factors, including Ku70 and Ku80 have additional functions outside of NHEJ (e.g. at telomere ends) (40), whether reducing their activities might also preclude A-EJ or other DSB repair mechanisms in human disease remains to be explored. By contrast, in the complete absence of Lig4 and other canonical NHEJ factors (Xrcc4, Ku70 and Ku80), CSR exclusively utilizes MH joining catalyzed by A-EJ as the DSB repair pathway of choice (3, 26, 32). Our data provides definitive evidence that residual, functional NHEJ DSB end-joining is highly error-prone, as demonstrated by the high frequency of IgH breaks and translocations in α-CD40+IL4 stimulated Lig4$^{R/R}$HL B-lymphocytes that also underwent robust IgG1 and IgE switching. Whereas the evidence of only residual A-EJ activity in LPS +α-IgD activated Lig4$^{R/R}$HL B-lymphocyte cultures, which resulted in equally high levels of IgH breaks and translocations as in the α-CD40+IL4 cultures, negated the possibility of a major role for A-EJ in error-prone repair within this Lig4 mutation.

Recent evidence suggested NHEJ instead of A-EJ as the cause of oncogenic translocations that arise in human cells (41). Our findings demonstrate that error-prone NHEJ via mutant Lig4^{R278H} activity can create translocations in murine mature B-lymphocytes, but brings into question as to whether the resulting translocations versus those generated by A-EJ when NHEJ is completely absent can oncogenically progress. In contrast the impact of p53-deficiency in Lig4-deficient or Xrcc4-deficient mature B-lymphocyte, cellular p53 status neither increased survival nor significantly influenced the frequency of IgH locus chromosomal breaks and translocations of activated Lig4$^{R/R}$HLp53$^{-/-}$ B-lymphocytes, or their malignant transformation *in vivo*. This may be because the accumulated damage to cells may be too extensive to propagate. This provides a plausible explanation as to why splenic B-lymphocytes in Lig4$^{R/R}$HL mice are highly prone to cell death even in the p53-

deficient setting; and in a subset of RS-SCID Lig4 patients (with compound heterozygote truncating mutations, e.g., R814X; K424Rfs20X) in whom residual Lig4 activity were retained, as to why serum IgA levels are so severely reduced (11, 17, 42). Whereas for *LIG4* mutations in which both Lig4 expression and activity are severely impaired, increased A-EJ access to AID-induced DSBs in Sμ and Sα regions could explain the relatively mild IgA switching defect in patients that exhibit a near null Lig4 phenotype (e.g., such as in patients with compound heterozygote truncating c.613delT and c.1904delA mutations (16)). Severely reduced Lig4 protein levels and increased A-EJ access could also explain the near normal serum IgA in $Lig4^{Y288C/Y288C}$ mice (35).

Our characterization of the impact of the Lig4R278H activity using the $Lig4^{R/R}$ model demonstrates how CSR junctions are resolved when NHEJ factors are intact but have only residual DSB repair activity. That intact Lig4 and NHEJ levels, regardless of functional Lig4 end-ligation activity, restricts A-EJ access to AID substrates. In the context general DSB repair, the mutant $Lig4^{R278H}$-NHEJ activity continues to protect/guard unrepaired DSBs from A-EJ. A consequence of this action is cumulated DNA damage too extensive to be repaired, which could explain the more general phenotypic outcomes, including growth retardation and severe radiosensitivity of $Lig4^{R/R}$ mice. The more general impacts of this and other *LIG4* mutations on DNA damage response could further explain the clinical phenotypic overlap of Lig4 Syndrome and Nijmegen Breakage Syndrome patients.

These overall findings explain why in contrast to patients with other NHEJ mutations, including in *ARTEMIS*, all Lig4 patient alleles are hypomorphic and not completely null (42), and the spectrum and impact of the autosomal inherited Lig4 mutations identified to date. Our findings suggest Lig4 plays a critical role in A-EJ suppression. Hence a key function of Lig4-NHEJ to ensure normal development growth, immune function and genome stability, is to actively guard cells from the aberrant consequence of A-EJ, which our findings suggest is normally highly restricted. These data predicts hypomorphic *LIG4* mutations impair B-lymphopoiesis via error-prone NHEJ and A-EJ suppression, and suggest survival advantage conferred by increased A-EJ activity underscores the wide diversity of genomic instability and cancer predisposition in Lig4 patients. Together these combined effects could explain the diverse, complex pathological consequences of germline and somatic mutations in NHEJ in human disease.

Supplementary Material

Refer to Web version on PubMed Central for supplementary material.

Acknowledgments

We thank Lauren Feldman for technical help on flow cytometry, PCR and sequencing, and analysis of CSR joins.

References

1. Dudley DD, Chaudhuri J, Bassing CH, Alt FW. Mechanism and control of V(D)J recombination versus class switch recombination: similarities and differences. Advances in immunology. 2005; 86:43–112. [PubMed: 15705419]

2. Chaudhuri J, Basu U, Zarrin A, Yan C, Franco S, Perlot T, Vuong B, Wang J, Phan RT, Datta A, Manis J, Alt FW. Evolution of the immunoglobulin heavy chain class switch recombination mechanism. Advances in immunology. 2007; 94:157–214. [PubMed: 17560275]

3. Yan CT, Boboila C, Souza EK, Franco S, Hickernell TR, Murphy M, Gumaste S, Geyer M, Zarrin AA, Manis JP, Rajewsky K, Alt FW. IgH class switching and translocations use a robust non-classical end-joining pathway. Nature. 2007; 449:478–482. [PubMed: 17713479]

4. Frank KM, Sekiguchi JM, Seidl KJ, Swat W, Rathbun GA, Cheng HL, Davidson L, Kangaloo L, Alt FW. Late embryonic lethality and impaired V(D)J recombination in mice lacking DNA ligase IV. Nature. 1998; 396:173–177. [PubMed: 9823897]

5. Plowman PN, Bridges BA, Arlett CF, Hinney A, Kingston JE. An instance of clinical radiation morbidity and cellular radiosensitivity, not associated with ataxia-telangiectasia. The British journal of radiology. 1990; 63:624–628. [PubMed: 2400879]

6. Riballo E, Critchlow SE, Teo SH, Doherty AJ, Priestley A, Broughton B, Kysela B, Beamish H, Plowman N, Arlett CF, Lehmann AR, Jackson SP, Jeggo PA. Identification of a defect in DNA ligase IV in a radiosensitive leukaemia patient. Curr Biol. 1999; 9:699–702. [PubMed: 10395545]

7. Ben-Omran TI, Cerosaletti K, Concannon P, Weitzman S, Nezarati MM. A patient with mutations in DNA Ligase IV: clinical features and overlap with Nijmegen breakage syndrome. American journal of medical genetics. 2005; 137A:283–287. [PubMed: 16088910]

8. Toita N, Hatano N, Ono S, Yamada M, Kobayashi R, Kobayashi I, Kawamura N, Okano M, Satoh A, Nakagawa A, Ohshima K, Shindoh M, Takami T, Kobayashi K, Ariga T. Epstein-Barr virus-associated B-cell lymphoma in a patient with DNA ligase IV (LIG4) syndrome. American journal of medical genetics. 2007; 143:742–745. [PubMed: 17345618]

9. O'Driscoll M, Cerosaletti KM, Girard PM, Dai Y, Stumm M, Kysela B, Hirsch B, Gennery A, Palmer SE, Seidel J, Gatti RA, Varon R, Oettinger MA, Neitzel H, Jeggo PA, Concannon P. DNA ligase IV mutations identified in patients exhibiting developmental delay and immunodeficiency. Molecular cell. 2001; 8:1175–1185. [PubMed: 11779494]

10. Unal S, Cerosaletti K, Uckan-Cetinkaya D, Cetin M, Gumruk F. A novel mutation in a family with DNA ligase IV deficiency syndrome. Pediatric blood & cancer. 2009; 53:482–484. [PubMed: 19418549]

11. Murray JE, Bicknell LS, Yigit G, Duker AL, van Kogelenberg M, Haghayegh S, Wieczorek D, Kayserili H, Albert MH, Wise CA, Brandon J, Kleefstra T, Warris A, van der Flier M, Bamforth JS, Doonanco K, Ades L, Ma A, Field M, Johnson D, Shackley F, Firth H, Woods CG, Nurnberg P, Gatti RA, Hurles M, Bober MB, Wollnik B, Jackson AP. Extreme growth failure is a common presentation of ligase IV deficiency. Human mutation. 2014; 35:76–85. [PubMed: 24123394]

12. Grunebaum E, Bates A, Roifman CM. Omenn syndrome is associated with mutations in DNA ligase IV. The Journal of allergy and clinical immunology. 2008; 122:1219–1220. [PubMed: 18845326]

13. Opitz JM, Pfeiffer RA, Hermann JP, Kushnick T. Studies of malformation syndromes of man XXIV B: the Dubowitz syndrome. Further observations. Zeitschrift fur Kinderheilkunde. 1973; 116:1–12. [PubMed: 4771703]

14. Yue J, Lu H, Lan S, Liu J, Stein MN, Haffty BG, Shen Z. Identification of the DNA repair defects in a case of Dubowitz syndrome. PloS one. 2013; 8:e54389. [PubMed: 23372718]

15. van der Burg M, van Veelen LR, Verkaik NS, Wiegant WW, Hartwig NG, Barendregt BH, Brugmans L, Raams A, Jaspers NG, Zdzienicka MZ, van Dongen JJ, van Gent DC. A new type of radiosensitive T-B-NK+ severe combined immunodeficiency caused by a LIG4 mutation. The Journal of clinical investigation. 2006; 116:137–145. [PubMed: 16357942]

16. H IJ, Warris A, van der Flier M, Reisli I, Keles S, Chishimba S, van Dongen JJ, van Gent DC, van der Burg M. Clinical spectrum of LIG4 deficiency is broadened with severe dysmaturity, primordial dwarfism, and neurological abnormalities. Human mutation. 2013; 34:1611–1614. [PubMed: 24027040]

17. Enders A, Fisch P, Schwarz K, Duffner U, Pannicke U, Nikolopoulos E, Peters A, Orlowska-Volk M, Schindler D, Friedrich W, Selle B, Niemeyer C, Ehl S. A severe form of human combined immunodeficiency due to mutations in DNA ligase IV. J Immunol. 2006; 176:5060–5068. [PubMed: 16585603]

18. Pan-Hammarstrom Q, Jones AM, Lahdesmaki A, Zhou W, Gatti RA, Hammarstrom L, Gennery AR, Ehrenstein MR. Impact of DNA ligase IV on nonhomologous end joining pathways during class switch recombination in human cells. The Journal of experimental medicine. 2005; 201:189–194. [PubMed: 15657289]
19. Riballo E, Doherty AJ, Dai Y, Stiff T, Oettinger MA, Jeggo PA, Kysela B. Cellular and biochemical impact of a mutation in DNA ligase IV conferring clinical radiosensitivity. The Journal of biological chemistry. 2001; 276:31124–31132. [PubMed: 11349135]
20. Bryans M, Valenzano MC, Stamato TD. Absence of DNA ligase IV protein in XR-1 cells: evidence for stabilization by XRCC4. Mutation research. 1999; 433:53–58. [PubMed: 10047779]
21. Rucci F, Notarangelo LD, Fazeli A, Patrizi L, Hickernell T, Paganini T, Coakley KM, Detre C, Keszei M, Walter JE, Feldman L, Cheng HL, Poliani PL, Wang JH, Balter BB, Recher M, Andersson EM, Zha S, Giliani S, Terhorst C, Alt FW, Yan CT. Homozygous DNA ligase IV R278H mutation in mice leads to leaky SCID and represents a model for human LIG4 syndrome. Proceedings of the National Academy of Sciences of the United States of America. 2010; 107:3024–3029. [PubMed: 20133615]
22. Frank KM, Sharpless NE, Gao Y, Sekiguchi JM, Ferguson DO, Zhu C, Manis JP, Horner J, DePinho RA, Alt FW. DNA ligase IV deficiency in mice leads to defective neurogenesis and embryonic lethality via the p53 pathway. Molecular cell. 2000; 5:993–1002. [PubMed: 10911993]
23. Sonoda E, Pewzner-Jung Y, Schwers S, Taki S, Jung S, Eilat D, Rajewsky K. B cell development under the condition of allelic inclusion. Immunity. 1997; 6:225–233. [PubMed: 9075923]
24. Pelanda R, Schwers S, Sonoda E, Torres RM, Nemazee D, Rajewsky K. Receptor editing in a transgenic mouse model: site, efficiency, and role in B cell tolerance and antibody diversification. Immunity. 1997; 7:765–775. [PubMed: 9430222]
25. Donehower LA, Harvey M, Slagle BL, McArthur MJ, Montgomery CA Jr, Butel JS, Bradley A. Mice deficient for p53 are developmentally normal but susceptible to spontaneous tumours. Nature. 1992; 356:215–221. [PubMed: 1552940]
26. Boboila C, Jankovic M, Yan CT, Wang JH, Wesemann DR, Zhang T, Fazeli A, Feldman L, Nussenzweig A, Nussenzweig M, Alt FW. Alternative end-joining catalyzes robust IgH locus deletions and translocations in the combined absence of ligase 4 and Ku70. Proceedings of the National Academy of Sciences of the United States of America. 2010; 107:3034–3039. [PubMed: 20133803]
27. Jones KR, Gewirtz DA, Yannone SM, Zhou S, Schatz DG, Valerie K, Povirk LF. Radiosensitization of MDA-MB-231 breast tumor cells by adenovirus-mediated overexpression of a fragment of the XRCC4 protein. Molecular cancer therapeutics. 2005; 4:1541–1547. [PubMed: 16227403]
28. Park JH, Park EJ, Hur SK, Kim S, Kwon J. Mammalian SWI/SNF chromatin remodeling complexes are required to prevent apoptosis after DNA damage. DNA repair. 2009; 8:29–39. [PubMed: 18822392]
29. Ehrenstein MR, Rada C, Jones AM, Milstein C, Neuberger MS. Switch junction sequences in PMS2-deficient mice reveal a microhomology-mediated mechanism of Ig class switch recombination. Proceedings of the National Academy of Sciences of the United States of America. 2001; 98:14553–14558. [PubMed: 11717399]
30. Boboila C, Oksenych V, Gostissa M, Wang JH, Zha S, Zhang Y, Chai H, Lee CS, Jankovic M, Saez LM, Nussenzweig MC, McKinnon PJ, Alt FW, Schwer B. Robust chromosomal DNA repair via alternative end-joining in the absence of X-ray repair cross-complementing protein 1 (XRCC1). Proceedings of the National Academy of Sciences of the United States of America. 2012; 109:2473–2478. [PubMed: 22308491]
31. Franco S, Gostissa M, Zha S, Lombard DB, Murphy MM, Zarrin AA, Yan C, Tepsuporn S, Morales JC, Adams MM, Lou Z, Bassing CH, Manis JP, Chen J, Carpenter PB, Alt FW. H2AX prevents DNA breaks from progressing to chromosome breaks and translocations. Molecular cell. 2006; 21:201–214. [PubMed: 16427010]
32. Boboila C, Yan C, Wesemann DR, Jankovic M, Wang JH, Manis J, Nussenzweig A, Nussenzweig M, Alt FW. Alternative end-joining catalyzes class switch recombination in the absence of both Ku70 and DNA ligase 4. The Journal of experimental medicine. 2010; 207:417–427. [PubMed: 20142431]

33. Lansford R, Manis JP, Sonoda E, Rajewsky K, Alt FW. Ig heavy chain class switching in Rag-deficient mice. International immunology. 1998; 10:325–332. [PubMed: 9576620]
34. Cheng HL, Vuong BQ, Basu U, Franklin A, Schwer B, Astarita J, Phan RT, Datta A, Manis J, Alt FW, Chaudhuri J. Integrity of the AID serine-38 phosphorylation site is critical for class switch recombination and somatic hypermutation in mice. Proceedings of the National Academy of Sciences of the United States of America. 2009; 106:2717–2722. [PubMed: 19196992]
35. Nijnik A, Dawson S, Crockford TL, Woodbine L, Visetnoi S, Bennett S, Jones M, Turner GD, Jeggo PA, Goodnow CC, Cornall RJ. Impaired lymphocyte development and antibody class switching and increased malignancy in a murine model of DNA ligase IV syndrome. The Journal of clinical investigation. 2009; 119:1696–1705. [PubMed: 19451691]
36. Callen E, Jankovic M, Difilippantonio S, Daniel JA, Chen HT, Celeste A, Pellegrini M, McBride K, Wangsa D, Bredemeyer AL, Sleckman BP, Ried T, Nussenzweig M, Nussenzweig A. ATM prevents the persistence and propagation of chromosome breaks in lymphocytes. Cell. 2007; 130:63–75. [PubMed: 17599403]
37. Han JH, Akira S, Calame K, Beutler B, Selsing E, Imanishi-Kari T. Class switch recombination and somatic hypermutation in early mouse B cells are mediated by B cell and Toll-like receptors. Immunity. 2007; 27:64–75. [PubMed: 17658280]
38. Wang JH, Gostissa M, Yan CT, Goff P, Hickernell T, Hansen E, Difilippantonio S, Wesemann DR, Zarrin AA, Rajewsky K, Nussenzweig A, Alt FW. Mechanisms promoting translocations in editing and switching peripheral B cells. Nature. 2009; 460:231–236. [PubMed: 19587764]
39. Pan-Hammarstrom Q, Zhao Y, Hammarstrom L. Class switch recombination: a comparison between mouse and human. Advances in immunology. 2007; 93:1–61. [PubMed: 17383538]
40. Celli GB, Denchi EL, de Lange T. Ku70 stimulates fusion of dysfunctional telomeres yet protects chromosome ends from homologous recombination. Nature cell biology. 2006; 8:885–890.
41. Ghezraoui H, Piganeau M, Renouf B, Renaud JB, Sallmyr A, Ruis B, Oh S, Tomkinson AE, Hendrickson EA, Giovannangeli C, Jasin M, Brunet E. Chromosomal translocations in human cells are generated by canonical nonhomologous end-joining. Molecular cell. 2014; 55:829–842. [PubMed: 25201414]
42. Buck D, Moshous D, de Chasseval R, Ma Y, le Deist F, Cavazzana-Calvo M, Fischer A, Casanova JL, Lieber MR, de Villartay JP. Severe combined immunodeficiency and microcephaly in siblings with hypomorphic mutations in DNA ligase IV. European journal of immunology. 2006; 36:224–235. [PubMed: 16358361]

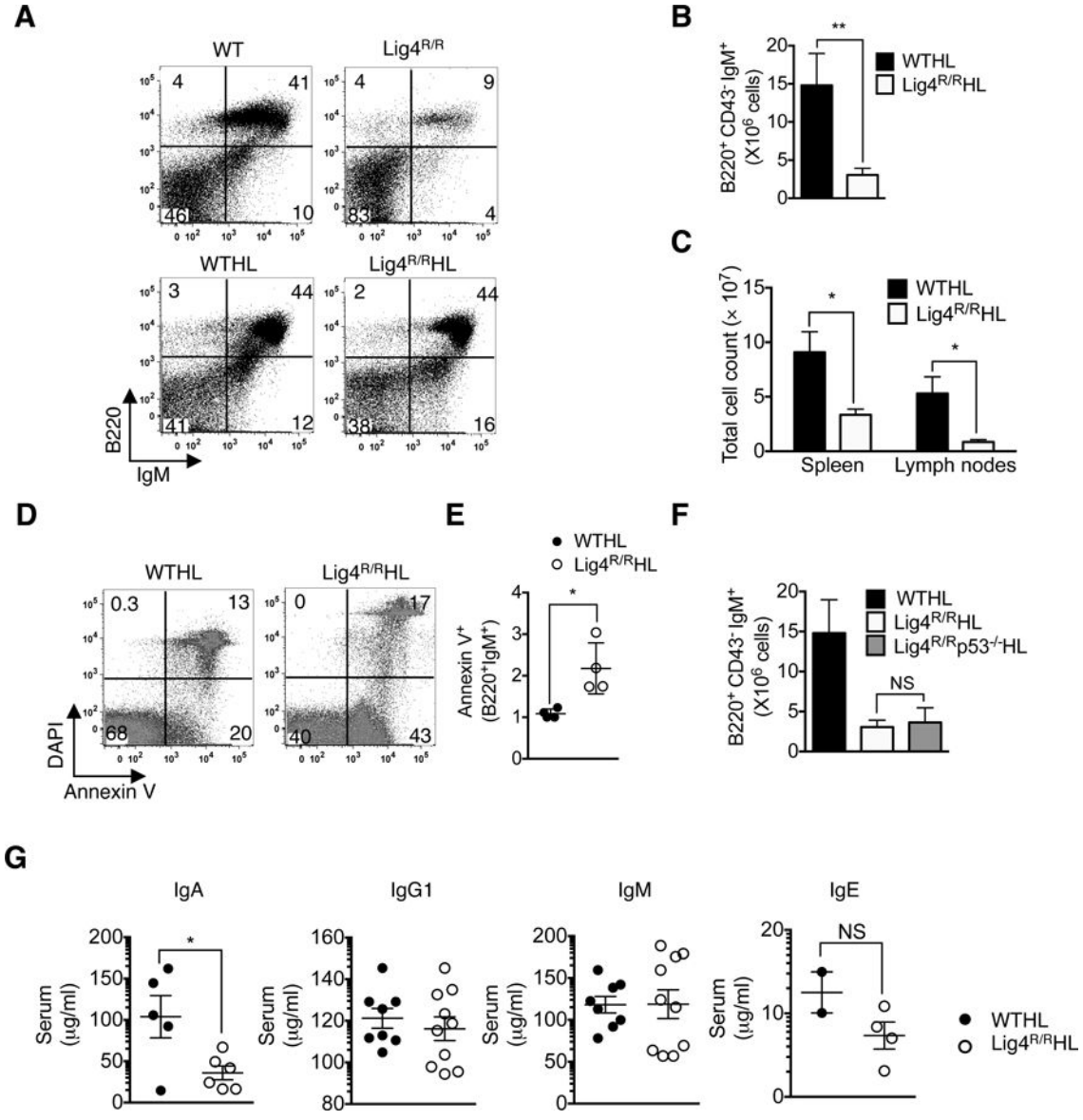

Figure 1. Introduction of HL knock-in alleles but not deficiencies in p53 partially rescues the mature B cell compartment in Lig4$^{R/R}$ mice

(A) Partial rescue of mutant B220^{+}CD43^{-}IgM^{+} B cell numbers by the HL knock-in. Representative B220 vs. IgM flow data from isolated splenocytes from age-matched WTHL and Lig4$^{R/R}$HL mice are shown. (**B**) Quantification of the total numbers of WTHL and Lig4$^{R/R}$HL splenic B220^{+}CD43^{-}IgM^{+} B cells, subsequent to red blood cell (RBC) lysis, column purification using CD43^{-} selection and flow cytometry (n=5; **p ≤ 0.01). (**C**) Total cell counts from splenic and mesenteric lymph nodes from Lig4$^{R/R}$HL and WTHL mice, quantified with Trypan Blue to exclude dead cells (n=3; *p ≤ 0.05). **(D–E)** Increased apoptosis in splenic B220^{+}IgM^{+} cells in the Lig4$^{R/R}$HL mice (**D**) Representative flow data of isolated splenocytes, gated on B220^{+}IgM^{+} cells and stained for Annexin-V and DAPI, are shown. **(E)** Percent quantification of overall Annexin-V^{+} cells is shown (n=5; *p ≤ 0.05). (**F**) No rescue of mutant B220^{+}CD43^{-}IgM^{+} B cell numbers by p53-deficiency. Total

$B220^{+}CD43^{-}IgM^{+}$ B cell numbers from WTHL, $Lig4^{R/R}$HL and $Lig4^{R/R}p53^{-/-}$HL mice were quantified. (n=4; NS, not significant [$Lig4^{R/R}$HL versus $Lig4^{R/R}p53^{-/-}$HL]). (**G**) Ig serum levels in WTHL and $Lig4^{R/R}$HL mice. Serum from 5–7-week-old WTHL and $Lig4^{R/R}$HL mice were collected and quantified by ELISA. (n=4; *$p \leq 0.05$; NS, not significant)

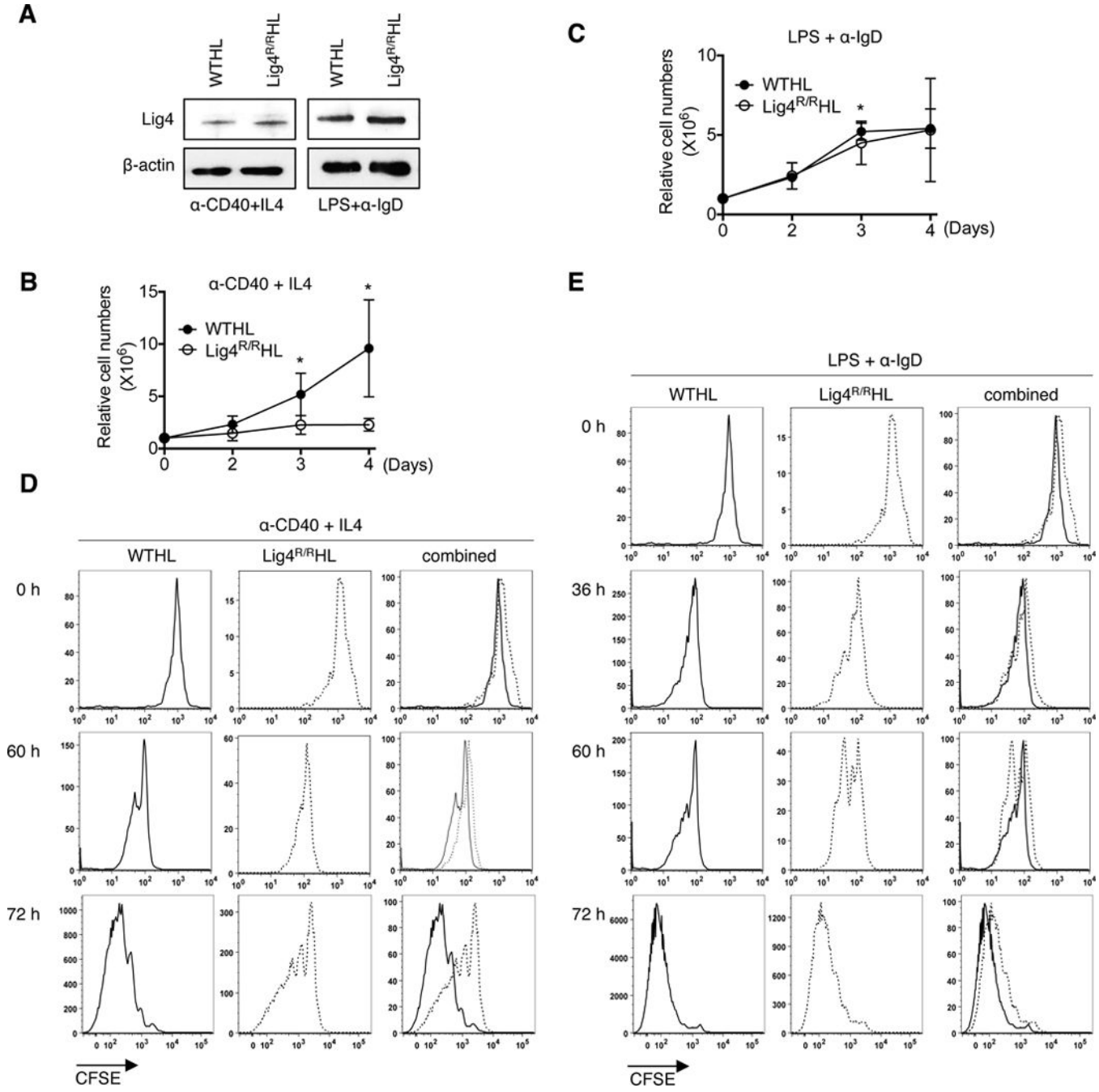

Figure 2. Impaired proliferation of Lig4$^{R/R}$HL B cells in α-CD40+IL4 but not in LPS+α-IgD activation

(A) Normal levels of Lig4 protein expression in activated Lig4$^{R/R}$HL B cells. Day 4 (96 h) α-CD40+IL4 and LPS+α-IgD activated WTHL and Lig4$^{R/R}$HL B cells were subjected to western blot analysis for the indicated proteins. Data is representative of three independent experiments. **(B–E)** Impaired proliferation rate/cycling in α-CD40+IL4 but not LPS+α-IgD activated Lig4$^{R/R}$HL B cells. **(B–C)** Daily cell counts with Trypan Blue exclusion of dead cells were graphed (n=5; P values calculated by Two-way ANOVA with Šídák; method; n=5; *p ≤ 0.05). **(D–E)** FACS plots show tracking of CFSE dilution in activated WTHL

(solid line) and Lig4$^{R/R}$HL B cells (dashed line) assayed at the indicated time points. Each peak progressing from right to left in the histogram indicates a cell division (n=3).

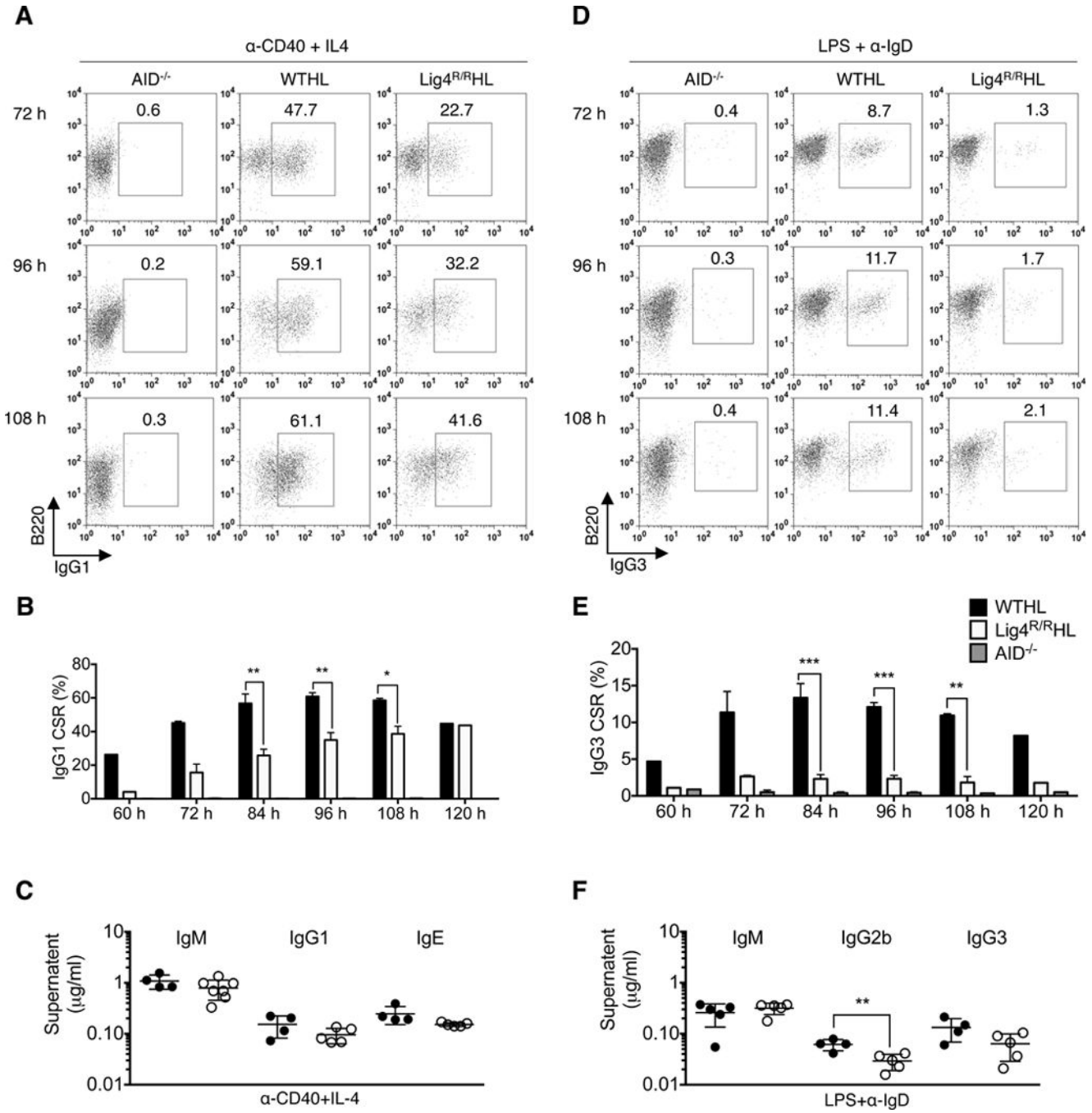

Figure 3. Slower kinetics but near optimal IgG1 class switching but severely impaired IgG3 switching in Lig4$^{R/R}$HL B cells

Class switching to IgG1 **(A–C)** and IgG3 **(D–F)** respectively in α-CD40+IL4 and LPS+α-IgD activated B cells from WTHL and Lig4$^{R/R}$HL littermates, and AID$^{-/-}$ mice (negative control). Surface Ig expression was assayed by flow cytometry at 12 h intervals from 60 h to 120 h of activation. **(A and D)** Representative flow data for surface IgG1 and IgG3 staining from cells harvested at 72 h, 96 h and 108 h are respectively shown. **(B and E)** Percentages of switching at each 12 h interval from 60–120 h were graphed (n=5; *p ≤ 0.05; **p ≤ 0.01;

***p ≤ 0.001[WTHL versus Lig4$^{R/R}$HL]) **(C and F)** Supernatant Ig levels. Supernatants from α-CD40+IL4 or LPS+α-IgD WTHL and Lig4$^{R/R}$HL B cell cultures wre collected at 96 h post-activation and quantified by ELISA (n=4; **p ≤ 0.01).

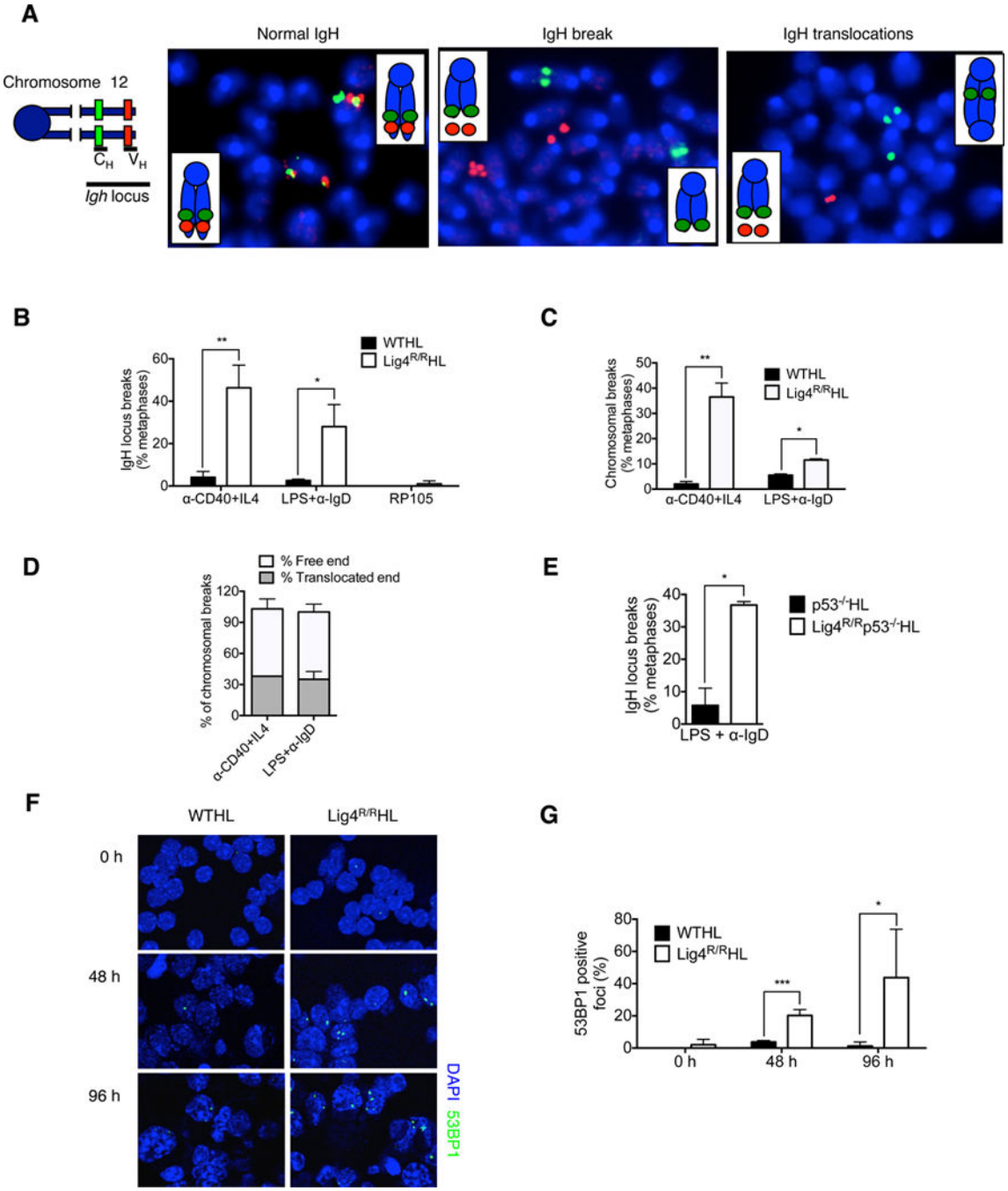

Figure 4. Frequent IgH-locus specific breaks and translocations, and persistence of 53BP1 foci in Lig4$^{R/R}$HL B cells

(A–D) Metaphases from day 4 (96 h) α-CD40+IL4, LPS+α-IgD or RP105 activated Lig4$^{R/R}$HL and control (WTHL) B cells analyzed by IgH FISH and T-FISH. **(A)** Schematic diagram of 3′IgH BAC probe (green) and 5′IgH BAC probe (red) (Left); and representative examples of metaphase FISH showing normal IgH loci, and IgH locus-specific chromosomal breaks and translocations in Lig4$^{R/R}$HL B cell cultures (Right) are shown. Nuclei were visualized by DAPI staining. **(B)** Percentage of IgH-specific breaks quantified

respectively (n=3; *p ≤ 0.05; **p ≤ 0.01). **(C)** Quantification of overall DNA breaks detected using a telomere-specific probe is shown (n=3; *p ≤ 0.05; **p ≤ 0.01). **(D)** Quantification of IgH translocation in $Lig4^{R/R}$HL B cells activated with α-CD40+IL4 or LPS+α-IgD. Percent translocation free (clear bars) versus translocation (filled bars) is shown (n=3), and further detailed in Table 1. **(E)** Quantification of overall IgH locus-specific breaks in Day 4 LPS+α-IgD activated $Lig4^{R/R}p53^{-/-}$HL and control ($p53^{-/-}$HL) B cells is shown (n=3; *p ≤ 0.05). **(F and G)** Increased levels of 53BP1 positive foci (as indicator of NHEJ activity) induced during CSR in α-CD40+IL4 activated $Lig4^{R/R}$HL B cells. Representative confocal images of 53BP1staining at 0 h, 48 h and 96 h of α-CD40+IL4 activation, with nuclei visualized by DAPI staining, is shown in **(F)**; and the summarized data is graphed in **(G).** (>150–200 cells were analyzed per condition; n=2; *p ≤ 0.05; ***p ≤ 0.001). Similar results were found in B cells activated with LPS+α-IgD (data not shown).

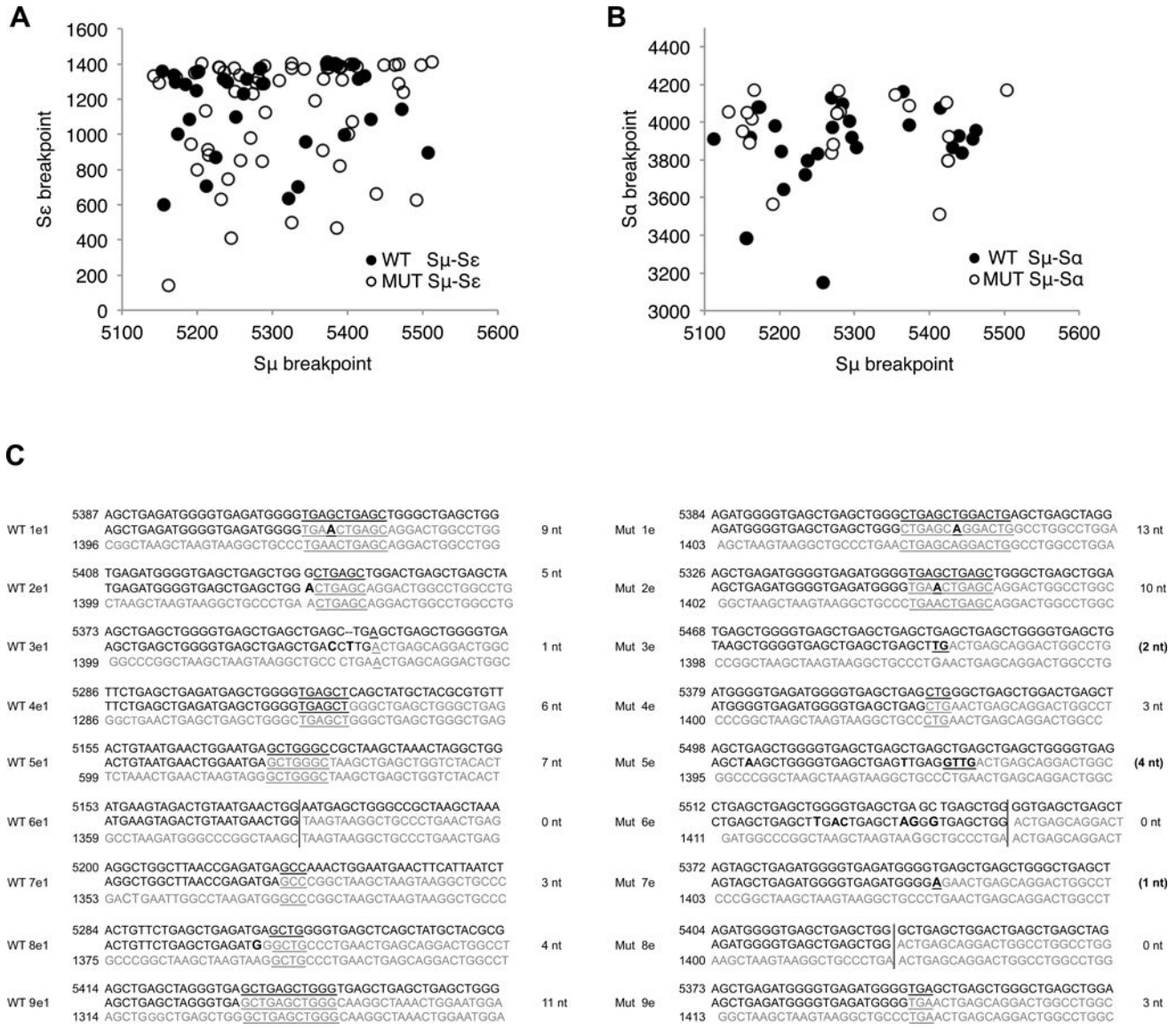

Figure 5. Normal distribution of switch junctions in activated Lig4$^{R/R}$HL B cells

(A) Distribution of Sμ-Sε junction breakpoints obtained from α-CD40+IL4 activated WTHL and Lig4$^{R/R}$HL B cells. Sequences shown: Sμ, top row; CSR junctions, middle row, and Sε, bottom row. **(B)** Distribution of Sμ-Sα switch junction breakpoints from splenic WT and Lig4$^{R/R}$ B cells. Sequences shown: Sμ, top row; CSR junctions, middle row, and Sα, bottom row. **(C)** Examples of WTHL and Lig4$^{R/R}$HL Sμ-Sε switch junctions. Germline IgH S region sequences obtained from Genbank: Sμ (MUSIGD07); Sε (MUSIGHAHX), and Sα (MUSIALPHA).

Microhomologies (MH) were identified as the longest region with perfect homology. Insertions were identified as sequences that lack any homology to either S region sequence. **Labeling:** WT, WTHL; MUT, Lig4$^{R/R}$HL. Nucleotide (nt) numbers for S region sequence files are shown to the left of the top and bottom sequences. Underlined text on top, middle and bottom rows designates MH nucleotide overlaps; bolded and underlined text in CSR junctions (middle row only) designates insertions; and bolded text in CSR junctions (middle

row only) denotes mutational changes. Vertical black line depicts direct/blunt joining of sequences that lack homology (no identity in either S region). Direct/blunt, MH nt overlaps and insertions (in parentheses) are noted the right of each sequence. These results are further detailed in Table 2.

Table 1

General and IgH breaks in α-CD40+IL4 and LPS+α-IgD activated Lig4$^{R/R}$HL B cells

		General genomic instability (T-FISH)			IgH locus-specific instability (IgH FISH)				
Genotype	**Cytokine**	**# metaphases analyzed**	**# metaphases with aberrations**	**total aberrations (%)**	**# metaphases analyzed**	**# metaphases with split 3′5′ IgH signal**	**# total IgH locus breaks (%)**	**# translocated IgH breaks/# total IgH locus breaks**	**# IgH locus breaks in dicentric/total # IgH locus breaks**
1st set of stimulations									
WTHL	α-CD40+IL4	90	1	1%	47	3	3 (6 %)	2/3 (66%)	0 (0 %)
	LPS+α-IgD	50	3	6%	44	1	1 (2 %)	1/1 (100%)	0 (0 %)
	RP105	ND	ND	ND	53	0	0 (0 %)	0 (0 %)	0 (0 %)
Lig4$^{R/R}$HL	α-CD40+IL4	24	10	42%	49	13	18 (37%)	3/18 (17%)	1/18 (5%)
	LPS+α-IgD	51	6	12%	51	7	8 (16%)	4/8 (50%)	1/8(12.5%)
	RP105	ND	ND	ND	53	1	1 (2 %)	1/1(100%)	0 (0 %)
2nd set of stimulations									
WTHL	α-CD40+IL4	34	1	3%	70	1	1 (1.4%)	0 (0 %)	0 (0 %)
	LPS+α-IgD	37	2	5%	50	3	3 (6%)	0 (0 %)	0 (0 %)
	RP105	ND	ND	ND	44	1	1 (2.3 %)	0 (0 %)	0 (0 %)
Lig4$^{R/R}$HL	α-CD40+IL4	35	11	31%	50	19	22 (44%)	11/22 (50%)	1/22 (5 %)
	LPS+α-IgD	46	5	11%	48	14	16 (33 %)	4/16 (25%)	0 (0 %)
	RP105	ND	ND	ND	43	0	0 (0 %)	0 (0 %)	0 (0 %)
3rd set of stimulations									
WTHL	α-CD40+IL4	50	0	0	83	2	2 (2.4 %)	0 (0 %)	0 (0 %)
	LPS+α-IgD	50	0	0	35	1	1 (3 %)	0 (0 %)	0 (0 %)
	RP105	ND	ND	ND	20	0	0 (0 %)	0 (0 %)	0 (0 %)
Lig4$^{R/R}$HL	α-CD40+IL4	120	55	46%	36	16	21 (58%)	8/21 (38%)	0 (0 %)
	LPS+α-IgD	ND	ND	ND	48	15	17 (35%)	5/17 (30%)	0 (0 %)

		General genomic instability (T-FISH)			IgH locus-specific instability (IgH FISH)				
Genotype	**Cytokine**	**# metaphases analyzed**	**# metaphases with aberrations**	**total aberrations (%)**	**# metaphases analyzed**	**# metaphases with split 3′5′ IgH signal**	**# total IgH locus breaks (%)**	**# translocated IgH breaks/# total IgH locus breaks**	**# IgH locus breaks in dicentric/total # IgH locus breaks**
	RP105	ND	ND	ND	32	1	1 (3.1 %)	0 (0 %)	0 (0 %)

* ND, Not determined

Table 2

CSR joins obtained from α-CD40+IL4 and LPS+α-IgD activated B cells

Switched Junctions	Stimulated B cells	Microhomology								Insertions				Total
		0	%	1 ~ 2	%	3 ~ 4	%	≥ 5	%	1 ~ 4	%	≥ 5	%	
Sμ-Sγ1	WT	5	20%	7	28%	6	24%	2	8%	3	12%	2	8%	25
	$Lig4^{R/R}$	6	20%	11	37%	8	27%	3	10%	1	3%	1	3%	30
Sμ-Sε	WT	5	16%	10	32%	9	29%	7	23%	0	0%	0	0%	31
	$Lig4^{R/R}$	12	18%	9	14%	19	29%	20	31%	3	5%	2	3%	65
Sμ-Sα	WT^{*}	8	27%	9	30%	5	17%	6	20%	2	7%	0	0%	30
	$Lig4^{R/R*}$	1	4%	4	17%	5	21%	12	50%	1	4%	1	4%	24

*PCR amplified directly from splenocytes. All analyzed sequences are shown in Supplemental Fig. 3.